

# Biological error correction codes generate fault-tolerant neural networks

Alexander Zlokapa,<sup>1,2</sup> Andrew K. Tan,<sup>3,2</sup> John M. Martyn,<sup>1,2</sup> Max Tegmark,<sup>3,2</sup> and Isaac L. Chuang<sup>3,4,2</sup>

<sup>1</sup>*Center for Theoretical Physics, Massachusetts Institute of Technology, Cambridge, MA 02139*

<sup>2</sup>*The NSF AI Institute for Artificial Intelligence and Fundamental Interactions*

<sup>3</sup>*Department of Physics, Massachusetts Institute of Technology, Cambridge, MA 02139*

<sup>4</sup>*Department of Electrical Engineering and Computer Science, Massachusetts Institute of Technology, Cambridge, MA 02139*

It has been an open question in deep learning if fault-tolerant computation is possible: can arbitrarily reliable computation be achieved using only unreliable neurons? In the mammalian cortex, analog error correction codes known as grid codes have been observed to protect states against neural spiking noise, but their role in information processing is unclear. Here, we use these biological codes to show that a universal fault-tolerant neural network can be achieved if the faultiness of each neuron lies below a sharp threshold, which we find coincides in order of magnitude with noise observed in biological neurons. The discovery of a sharp phase transition from faulty to fault-tolerant neural computation opens a path towards understanding noisy analog systems in artificial intelligence and neuroscience.

Early in the development of computer science, it was unknown if unreliable hardware would make the construction of reliable computers impossible. Whenever a component failed, the resulting error had to be corrected by additional components that were themselves likely to fail. Inspired by ideas from error correction, the notion of *fault-tolerant computation* resolved this issue in standard frameworks of classical and quantum computation [1–7]. In these settings, every computation is evaluated by a sequence of faulty components such as Boolean gates (e.g. AND, OR, NOT). If each component’s probability of failure falls below a sharp threshold, a strict criterion defining fault-tolerant computation is provably satisfied: computations of any length can be performed with arbitrarily low error.

Here, we consider a noisy neuron as the fundamental component of computation. In artificial intelligence, it is unresolved [8] if neural networks can satisfy the criterion of fault tolerance. In neuroscience, although observations of the mammalian brain show that neural *representations* are protected against analog noise [9–11], it is unknown if such error-correcting mechanisms are powerful enough to theoretically perform *computations* with arbitrarily small error. We resolve both open questions by demonstrating a phase transition into the regime of fault-tolerant neural computation using biological error correction codes.

We make the notion of fault tolerance precise through von Neumann’s original result for fault-tolerant Boolean formulas, which perform universal computation using Boolean gates [1]. Each gate in the original error-free formula is replaced by a *logical* gate composed of many *physical* gates that each fail with some fixed probability  $p$ . The logical gate is built with error correction such as the repetition code: data is repeated in bundles of three and majority voting determines the outcome. Despite the voting itself being performed by faulty physical gates, von Neumann showed via a recursive repetition code (see Supplementary Information Sec. I) that a fault-tolerant Boolean formula can be constructed if the failure probability  $p$  falls below some threshold  $p_0$ . In general,

the value of  $p_0$  depends on the model of computation under study [2–6], e.g. Ref. [4] demonstrated a noise threshold for reliable computation of  $p_0 = \frac{3-\sqrt{7}}{4} \approx 0.09$  for Boolean formulas constructed from 2-input NAND formulas, which are sufficient for universal computation. More broadly, the formal concepts of fault-tolerant computation and its associated threshold can be stated as follows:

**Digital fault tolerance.** A Boolean formula containing  $N$  (error-free) gates can be simulated with probability of error at most  $\epsilon$  using  $\mathcal{O}(N \log^b(N/\epsilon))$  faulty gates for some positive constant  $b$ . Each gate may fail with probability  $p$  for  $p < p_0$ , where  $p_0$  is independent of  $N$  and independent of the depth of the desired formula.

The digital computation setting of traditional fault tolerance strongly contrasts the *analog* computation paradigm of the brain, where neurons operate using continuous rather than discrete values. While synaptic failure of neurons produces digital-like errors [12, 13] that may be satisfactorily treated by an extension of von Neumann’s construction (Fig. 1), neurons also experience analog noise. The neural spiking of biological axon output is subject to additive Gaussian noise with a Fano factor of around one [14]. The dominant modes of noise are thus parameterized by two parameters: the probability  $p$  of synaptic failure, and the standard deviation  $\sigma$  of neural output. In a digital setting, a repetition code of size  $N$  exponentially suppresses errors in  $N$ . However, for  $N$  neurons in the presence of analog noise, repetition only reduces noise by  $\sigma/\sqrt{N}$ , rendering naive fault tolerance protocols inadequate (see Supplementary Information Sec. III).

To formalize the analog biological setting of computation, we adopt the framework of artificial neural networks, which have been shown to be universal approximators of continuous functions [15] and have experienced wide success in applications resembling cognitive

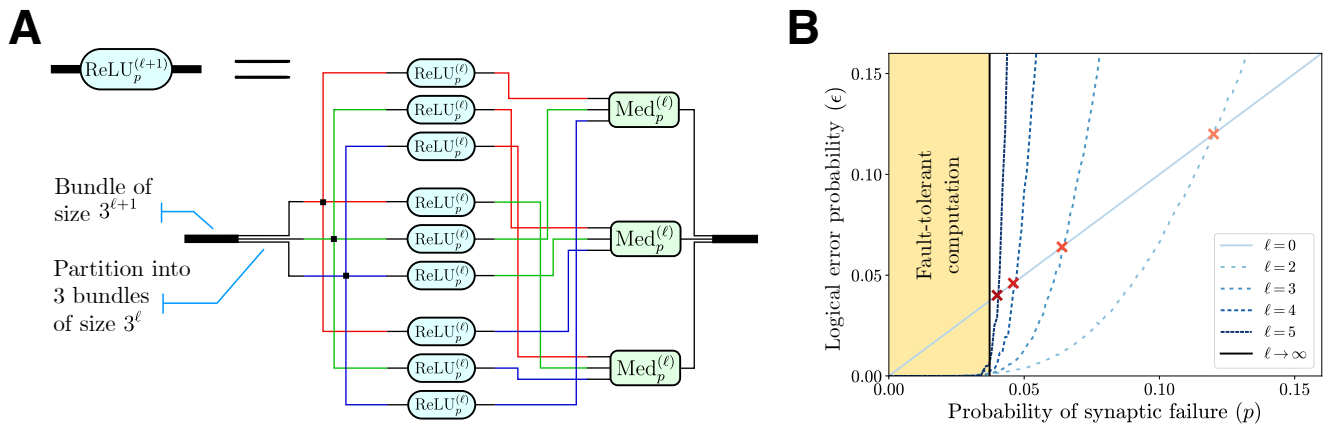


FIG. 1. (A) Logical activation function for a fault-tolerant neural network in the presence of synaptic failure. Focusing on a network with ReLU (rectified linear unit) activation functions  $\text{ReLU}(x) = \max(0, x)$ , we model synaptic failure through a faulty  $\text{ReLU}_p$  that outputs 0 with probability  $p$ . The recursive concatenation procedure of digital fault tolerance is extended to construct a logical ReLU at concatenation level  $\ell + 1$  (denoted  $\text{ReLU}_p^{(\ell+1)}$ ) from logical ReLUs at level  $\ell$ , with the base case  $\text{ReLU}_p^{(0)} = \text{ReLU}_p$ . The gates denoted  $\text{Med}_p^{(\ell)}$  indicate a median operation that is composed of  $\text{ReLU}_p^{(\ell)}$ s and used to correct errors (see Supplementary Information Sec. II). (B) The logical error probability of  $\text{ReLU}_p^{(\ell)}(x)$  on random inputs  $x \in [-1, 1]$  as determined by numerical simulation. The pseudothresholds (red crosses) occur when the error probability intersects that of  $\ell = 0$ ; they converge exponentially to the threshold  $p_0 \approx 3.72\%$  (vertical black line) with increasing  $\ell$ .

tasks [16]. Following biological inspiration [17], the standard artificial neuron takes input through synapses and passes output along an axon to subsequent neurons. The resilience of artificial neural networks to errors has been limited primarily to demonstrations of robustness to weight perturbations or other noise, and hardware fault tolerance in neuromorphic computing [18–23], without considering biologically-motivated noise nor addressing the formal notion of fault tolerance analogous to digital fault tolerance defined above.

We will ultimately prove the following result by using biological error-correcting mechanisms for neural computation:

**Neural network fault tolerance.** A Boolean formula of  $N$  (error-free) gates can be simulated by a neural network with probability of error at most  $\epsilon$  using only faulty neurons. The output of each neuron is subject to additive Gaussian noise with mean zero and variance  $\sigma^2$ ; each synapse entering a neuron fails with probability  $p$ ; a neuron admits at most a fixed number of synapses. There exist nonzero thresholds  $p_0$  and  $\sigma_0$  such that if  $p < p_0$  and  $\sigma < \sigma_0$ , simulating the formula requires  $\mathcal{O}(N \log(N/\epsilon))$  faulty neurons.

In particular, we employ biological error codes known as *grid codes* that have been experimentally demonstrated to successfully store error-corrected representations of states such as an animal’s location [10]. Unlike the repetition code, the grid code achieves exponentially small error at asymptotically finite information rates, saturating the Shannon bound [24] and allowing effective

error correction against Gaussian neural spiking noise.

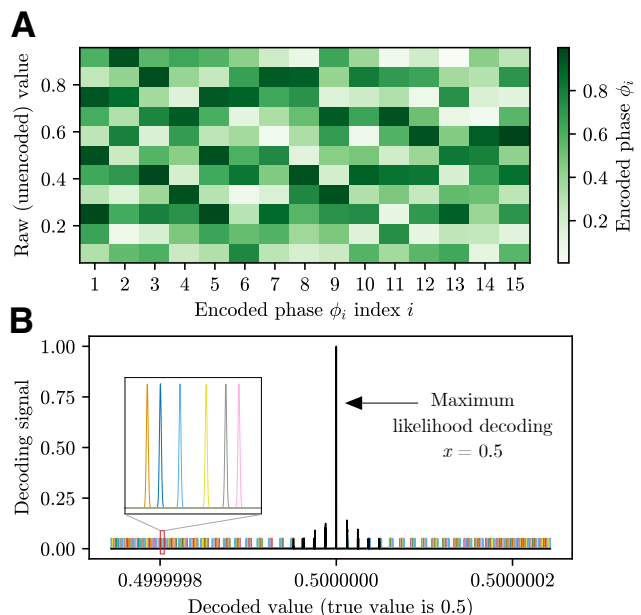


FIG. 2. (A) Example encoding performed by the grid code over  $M = 15$  moduli  $\{\lambda_1, \dots, \lambda_{15}\}$ . (B) Example decoding of phases representing  $x = 0.5$ . The possible decodings allowed by a given phase (indicated by a unique color for each  $\lambda_j$ ) are periodic. Each decoded phase is subject to Gaussian noise (inset). Since the phases constructively add at the true decoded value, maximum likelihood estimation is performed by selecting the decoded value with the highest signal.

Studies of the entorhinal cortex in mammals show that

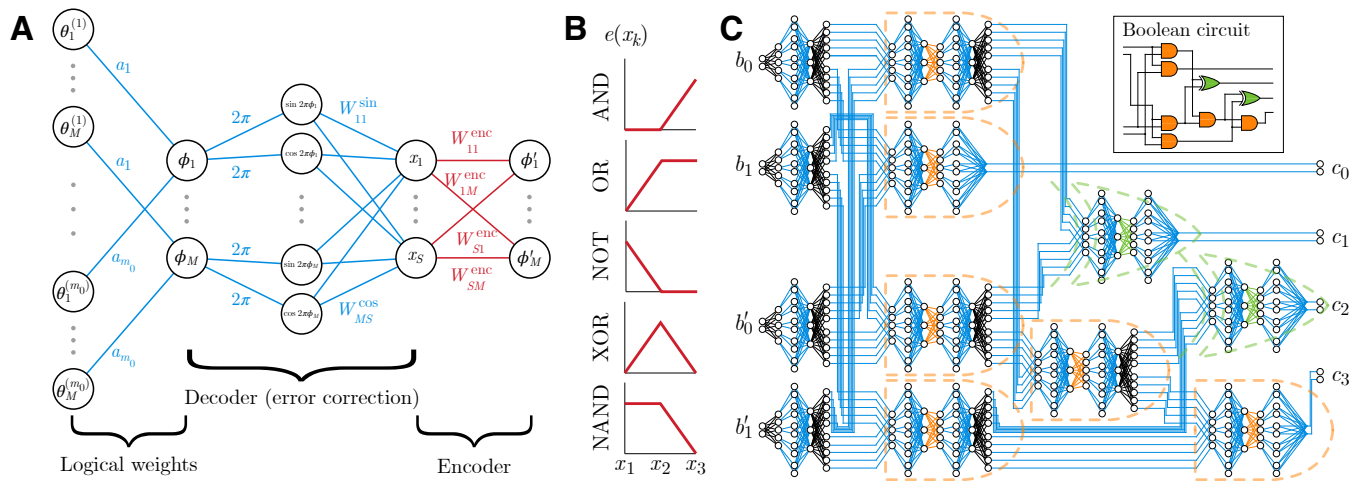


FIG. 3. (A) Logical neuron decomposed into physical neurons to achieve fault-tolerance in the presence of analog noise. The neuron receives encoded neural outputs from the previous layer and performs a computation with time advancing to the right. The logical weights  $a_i$  are applied in the codespace, and the decoder recovers  $x_k$  to perform error correction. The encoder (red) performs a logical activation function (e.g. ReLU) using appropriate weights back to the codespace. (B) Encoder functions  $e(x_k)$  that induce appropriate logical activation functions to implement common Boolean gates. All logical weights  $a_i$  are set to unity when implementing a Boolean gate. (C) Analog fault-tolerant neural network implementing multiplication, and the equivalent digital Boolean circuit (inset). Two 2-bit binary numbers  $b_0b_1$  and  $b'_0b'_1$  are one-hot encoded as input to the noisy neural network, and the output product  $c_0c_1c_2c_3$  may be estimated with arbitrarily small error by increasing the number of moduli ( $M = 5$  moduli illustrated). The grid code corrects Gaussian neural spiking noise in each logical neuron due to the decoder (blue); neural encoders evaluate AND gates (orange) and XOR gates (green) to perform computation using encoder activation functions (shown in B); additional decoders and encoders are used to generated error-corrected copies of neural states (black).

lattice neural firing patterns may correspond to the encoding of a given number  $x_k$  from a discrete set of possible values that lie within a fixed interval  $[0, X)$ . The grid cells represent a set of phases through the encoder

$$\text{Enc}[x_k] := \left\{ \frac{e(x_k)}{\lambda_j} \bmod 1 \right\}_{j=1}^M, \quad (1)$$

which is defined over  $M$  relatively prime integers  $\{\lambda_j\}_{j=1}^M$  referred to as *moduli* [9, 10]. In the original grid code,  $e(x_k)$  is chosen to be the identity, corresponding to a saw-tooth function that ultimately represents  $x_k$ . Here, we instead perform computation in the codespace by selecting  $e$  to perform a logical activation function. In general, we denote the vector of  $M$  phases produced by the encoder as  $\phi := \text{Enc}[x_k] = \{\phi_j\}$ .

In the limit  $\max_j \lambda_j \ll X$  for  $X \ll \prod_{j=1}^M \lambda_j$ , the phases are well-approximated as being drawn uniformly at random. This provides a sensitive encoding that changes significantly if the input is slightly perturbed (Fig. 2a). Since each codeword consists of a vector of phases with the period of each  $\phi_j$  determined by  $\lambda_j$ , decoding corresponds to the constructive interference of summed phases to yield the correct decoded position (Fig. 2b). This allows the encoder and decoder of a grid code to be implemented directly with a neural network, approximating maximum likelihood estimation over codewords.

An ideal decoder  $\text{Dec}[\phi]$  would perform maximum like-

lihood estimation (MLE) to recover the most probable  $x_{k_0}$  given a codeword  $\phi$ . For ease of presentation, we modify the original biologically inspired neural decoder that approximates MLE [11] to a simpler but functionally equivalent form. Given phases  $\phi = \{\phi_j\}$ , the true position  $x_{k_0}$  is recovered by the MLE decoder

$$\text{Dec}[\phi] := \arg \max_{x_k} \sum_{j=1}^M \cos \left[ 2\pi \left( \frac{x_k}{\lambda_j} - \phi_j \right) \right]. \quad (2)$$

To implement the MLE decoder with a neural network, the angle difference is decomposed via the standard identity  $\cos(\alpha - \beta) = \cos \alpha \cos \beta + \sin \alpha \sin \beta$ . To estimate  $\arg \max_{x_k}$ , we use a step activation function with a tuned threshold based on the number of moduli, replacing winner-take-all dynamics with a simpler localized activation function (see Supplementary Information Sec. VII). At the end of a successful decoding, the output neuron at index  $k_0$  will be one-hot encoded to have value 1 while all other output neurons will have value 0. However, noise will introduce imperfections: every neuron in the encoder and decoder are subjected to noise throughout every step of the error correction process, e.g.  $\bar{\text{Enc}}[x_k] := \{e(x_k)/\lambda_j + \xi_j \bmod 1\}$  for normally distributed  $\xi_j \sim \mathcal{N}(0, \sigma)$ .

We show fault tolerance for a neural network with Gaussian-distributed weights (see Supplementary Information Sec. V) as well as a neural network with

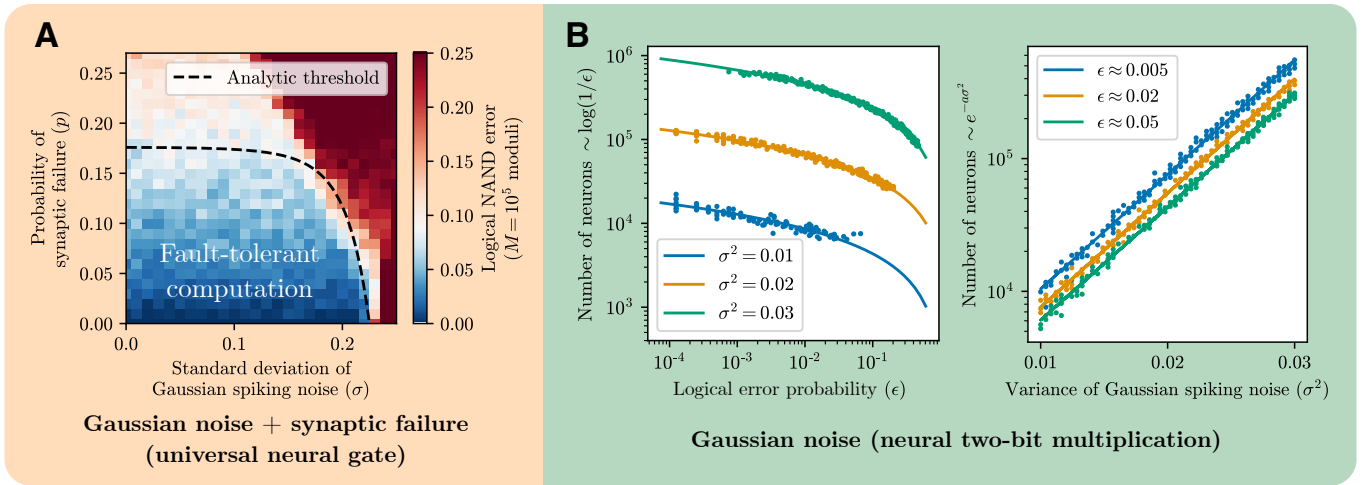


FIG. 4. (A) Fault tolerance threshold for a neural implementation of a universal Boolean gate (NAND gate). A sharp phase transition enables a fault-tolerant neural network to perform arbitrarily long computations with arbitrarily small error if the noise of each physical neuron (probability of synaptic failure and neural spiking noise) falls below the threshold. Regions in blue support fault-tolerant computation, while regions in red cause faulty computation. The color is determined by the logical NAND error probability  $\epsilon_0 \approx 0.09$  required to achieve an arbitrarily low logical error using the optimal NAND fault tolerance construction [4]. (B) Numerical simulation of the number of neurons required to perform two-bit multiplication with logical error probability  $\epsilon$  in the presence of Gaussian noise  $\sigma^2$  (and zero probability of synaptic failure). We confirm the analytic scaling  $\mathcal{O}(e^{a\sigma^2} N \log(N/\epsilon))$ .

weights and activation functions chosen to implement any Boolean formula (Supplementary Information Secs. V, VI). A *logical neuron* is formed by interleaving computations in the codespace with error correction to control the propagation of errors (Fig. 3a). The application of the decoder error-corrects the noisy codeword  $\tilde{\phi}$ , and the re-encoding completes the computation via the logical activation function. Explicitly, we project the set of encoded phases  $\tilde{\phi}$  back to codewords  $\tilde{\phi}' = \widetilde{\text{Enc}}[\widetilde{\text{Dec}}[\tilde{\phi}]]$ . Due to the cyclicity of the encoding from modular arithmetic, the phases  $\tilde{\phi}'$  represent a codeword corresponding to some  $x_k$  in a condensed codespace smaller than the original  $[0, X)$  space, generating a non-polynomial logical activation function that enables universal approximation of arbitrary continuous functions [15].

Here, unlike in the original grid code, the evaluation of  $\arg \max_{x_k}$  in the decoder may be evaluated over a set  $\{x_k\}$  that corresponds to a larger space than spanned by  $\text{Enc}[x_k]$ ; this active role in computation by the decoder will allow computation to take place directly between phases in the codespace via logical weights. Moreover, to remain protected against digital-like errors caused by synaptic failure, we will ultimately place the entire grid code within a concatenated repetition code; consequently, computation never leaves the codespace despite the presence of grid decoder blocks.

With i.i.d. Gaussian noise  $\xi \sim \mathcal{N}(0, \sigma)$  applied to the output of each physical neuron, the logical neuron is allowed to fail with probability  $\epsilon$  (the *logical error*). A careful treatment of the noise for Gaussian-distributed logical weights (see Supplementary Information Sec. V)

and neural implementations of the encoder and decoder (following Fig. 3a) shows that to leading order in  $\epsilon \ll 1$ , the number of moduli  $\lambda_j$  required to achieve a given logical error probability is

$$M(\epsilon) \approx e^{a\sigma^2} (1 + 2\sigma^2) \log(1/\epsilon), \quad (3)$$

where  $a$  is a constant independent of the noise or error correction overhead. The  $\mathcal{O}(e^{a\sigma^2})$  dependence on the spiking noise originates from the constructive interference of the grid code: noisy phases for the true decoding contribute to a neuron with mean activation  $Me^{-a\sigma^2/2}$ , while the incorrect decoding yields a mean activation of zero. Although the noise produces neural activations of variance  $\mathcal{O}(\sigma\sqrt{M})$ , there always exists sufficiently large  $M$  to identify the correct decoding. Hence, a fault-tolerant neural network can be constructed under the presence of arbitrarily large noise using  $\mathcal{O}(e^{a\sigma^2})$  physical neurons for constant  $a$ , if each physical neuron is allowed unbounded fan-in.

However, in biological networks, the highest neural connectivity is observed in Purkinje cells, which admit  $\sim 2 \times 10^5$  synapses [25]; to implement this fan-in constraint, we limit the number of moduli to  $10^5$ . Additionally, as discussed earlier, biological neurons also experience stochastic synaptic failure with some probability  $p$ . Both of these effects cause the logical neuron to fail with some fixed finite probability, which can be dealt with using standard fault tolerance techniques from classical computing. We use the logical neuron to construct standard Boolean gates by choosing the encoder function  $\epsilon(x_k)$  (Fig. 3b). Using the analysis of 2-input

NAND gates by Evans and Pippenger [4], we recover the fault tolerance threshold for arbitrary Boolean formulas by invoking the logical NAND neuron threshold of  $\epsilon_0 = (3 - \sqrt{7})/4 \approx 0.09$ .

We find a *phase transition* that describes the threshold for fault tolerance (Fig. 4a). In the lower region of logical error  $\epsilon < \epsilon_0$ , fault-tolerant computation is possible for Boolean formulas of arbitrary size; in the upper region of  $\epsilon > \epsilon_0$ , the fault-tolerant construction does not hold. Analytic estimates show the region of fault-tolerance is bounded by a synaptic failure probability of  $p_0 \approx 0.176$  and Gaussian neural spiking noise with standard deviation  $\sigma_0 \approx 0.225$  (see Supplementary Information Sec. VII); numerical simulation shows close agreement. We confirm that  $\mathcal{O}(N \log(N/\epsilon))$  neurons suffice (Fig. 4b, left) for fault tolerance through numerical simulation of fault-tolerant two-bit multiplication using neural AND and XOR gates (Fig. 3c); similarly, the  $\mathcal{O}(e^{a\sigma^2})$  neurons expected in the absence of connectivity constraints by Eq. 3 is numerically verified (Fig. 4b, right).

The fault-tolerant phase of computation agrees in order of magnitude with the extent of noise observed in biological neurons: the artificial neural network is fault-tolerant at  $p \approx 0.1$  and  $\sigma \approx 0.2$ , while biological neurons experience  $p \approx 0.5$  and  $\sigma \approx 1$  [12–14]. However, our result only places a lower bound on the fault-tolerance threshold; a more effective neural fault-tolerant construction may be possible. In particular, while the neural network fault tolerance theorem is phrased in terms of digital Boolean gates composed of analog neurons, Eq. 3 holds for a general construction of neural networks with Gaussian-distributed weights (see Supplementary Information Sec. V). This standard form of artificial neural networks provides a more direct analog approach to com-

putation without introducing logical digital gates, and it may ultimately realize a more efficient path towards a threshold for the fault-tolerant phase of neural computation.

Framed against the slowing pace of Moore’s Law and increasingly prohibitive energy costs of deep learning [26, 27], the efficiency of biological computation places central importance on a deep understanding of noisy analog systems. The brain is a canonical example of a noisy analog system that is more energy-efficient than traditional faultless computation; by demonstrating the existence of fault-tolerant neural networks, our work provides a concrete path towards leveraging the favorable properties of such analog neural networks in a neuromorphic setting [28–30]. In aggregate, these results are suggestive of the power of naturally occurring error-correcting mechanisms: while the presence of fault-tolerant computation in the brain remains uncertain, we conclude that experimentally observed neural error correction codes are sufficient to achieve arbitrarily reliable computation.

#### ACKNOWLEDGMENTS

The authors thank Ila Fiete for comments and discussion. AZ acknowledges support from the Hertz Foundation, and the Department of Defense through the National Defense Science and Engineering Graduate Fellowship Program. AKT acknowledges support from the Natural Sciences and Engineering Research Council of Canada (NSERC) [PGSD3-545841-2020]. MT acknowledges support from the Rothberg Family Fund for Cognitive Science. ILC, AKT, and MT acknowledge support in part from the Institute for Artificial Intelligence and Fundamental Interactions (IAIFI) through NSF Grant No. PHY-2019786.

- 
- [1] J. von Neumann, “Probabilistic logics and the synthesis of reliable organisms from unreliable components,” in *Automata Studies. (AM-34), Volume 34*, edited by C. E. Shannon and J. McCarthy (Princeton University Press, 2016) pp. 43–98.
  - [2] N. Pippenger, *26th Annual Symposium on Foundations of Computer Science (SFCS 1985)*, 30 (1985).
  - [3] B. Hajek and T. Weller, *IEEE Transactions on Information Theory* **37**, 388 (1991).
  - [4] W. Evans and N. Pippenger, *IEEE Transactions on Information Theory* **44**, 1299 (1998).
  - [5] W. Evans and L. Schulman, *IEEE Transactions on Information Theory* **45**, 2367 (1999).
  - [6] J. Gao, Y. Qi, and J. Fortes, *IEEE Transactions on Nanotechnology* **4**, 395 (2005).
  - [7] P. Shor, in *Proceedings of 37th Conference on Foundations of Computer Science* (1996) pp. 56–65.
  - [8] C. Torres-Huitzil and B. Girau, *IEEE Access* **5**, 17322 (2017).
  - [9] T. Hafting, M. Fyhn, S. Molden, M.-B. Moser, and E. I. Moser, *Nature* **436**, 801 (2005).
  - [10] I. R. Fiete, Y. Burak, and T. Brookings, *Journal of Neuroscience* **28**, 6858 (2008).
  - [11] S. Sreenivasan and I. Fiete, *Nature Neuroscience* **14**, 1330 (2011).
  - [12] C. F. Stevens and Y. Wang, *Nature* **371**, 704 (1994).
  - [13] N. A. Hessler, A. M. Shirke, and R. Malinow, *Nature* **366**, 569 (1993).
  - [14] W. Softky and C. Koch, *Journal of Neuroscience* **13**, 334 (1993).
  - [15] K. Hornik, M. Stinchcombe, and H. White, *Neural Networks* **2**, 359 (1989).
  - [16] Y. LeCun, Y. Bengio, and G. Hinton, *Nature* **521**, 436 (2015).
  - [17] W. S. McCulloch and W. Pitts, *The Bulletin of Mathematical Biophysics* **5**, 115 (1943).
  - [18] C. Neti, M. Schneider, and E. Young, *IEEE Transactions on Neural Networks* **3**, 14 (1992).
  - [19] E. M. El Mhamdi and R. Guerraoui, in *2017 IEEE International Parallel and Distributed Processing Symposium (IPDPS)* (2017) pp. 1028–1037.
  - [20] T. Liu, W. Wen, L. Jiang, Y. Wang, C. Yang, and

- G. Quan, in *2019 56th ACM/IEEE Design Automation Conference (DAC)* (2019) pp. 1–6.
- [21] C. Sequin and R. Clay, in *1990 IJCNN International Joint Conference on Neural Networks* (1990) pp. 703–708 vol.1.
- [22] C. Neti, M. Schneider, and E. Young, *IEEE Transactions on Neural Networks* **3**, 14 (1992).
- [23] U. Ruckert, I. Kreuzer, V. Tryba, and K. Goser, in *Proceedings. VLSI and Computer Peripherals. COMPEURO 89* (1989) pp. 1/52–1/55.
- [24] T. Gobblick, *IEEE Transactions on Information Theory* **11**, 558 (1965).
- [25] R. M. A. Napper and R. J. Harvey, *Journal of Comparative Neurology* **274**, 168 (1988).
- [26] T. B. Brown, B. Mann, N. Ryder, M. Subbiah, *et al.*, “Language models are few-shot learners,” (2020), [arXiv:2005.14165](https://arxiv.org/abs/2005.14165) [cs.CL].
- [27] J. Jumper, R. Evans, A. Pritzel, *et al.*, *Nature* **596**, 583 (2021).
- [28] G. Indiveri, B. Linares-Barranco, T. Hamilton, A. van Schaik, R. Etienne-Cummings, T. Delbruck, S.-C. Liu, P. Dudek, P. Häfliger, S. Renaud, J. Schemmel, G. Cauwenberghs, J. Arthur, K. Hynna, F. Folowosele, S. Saighi, T. Serrano-Gotarredona, J. Wijekoon, Y. Wang, and K. Boahen, *Frontiers in Neuroscience* **5**, 73 (2011).
- [29] S. K. Esser, P. A. Merolla, J. V. Arthur, A. S. Cassidy, R. Appuswamy, A. Andreopoulos, D. J. Berg, J. L. McKinstry, T. Melano, D. R. Barch, C. di Nolfo, P. Datta, A. Amir, B. Taba, M. D. Flickner, and D. S. Modha, *Proceedings of the National Academy of Sciences* **113**, 11441 (2016), <https://www.pnas.org/content/113/41/11441.full.pdf>.
- [30] Z. Wang, S. Joshi, S. Savel’ev, W. Song, R. Midya, Y. Li, M. Rao, P. Yan, S. Asapu, Y. Zhuo, H. Jiang, P. Lin, C. Li, J. H. Yoon, N. K. Upadhyay, J. Zhang, M. Hu, J. P. Strachan, M. Barnell, Q. Wu, H. Wu, R. S. Williams, Q. Xia, and J. J. Yang, *Nature Electronics* **1**, 137 (2018).

# Supplementary information for “Biological error-correction codes generate fault-tolerant neural networks

## CONTENTS

I. Digital fault tolerance via concatenated repetition code	1
II. Fault tolerance against synaptic failure via concatenated repetition code	1
III. Comparison of repetition for discrete versus analog fault-tolerance	2
IV. Summary of grid codes	3
V. Fault-tolerant Gaussian-weighted neural network	3
VI. Demonstration of Boolean gates with modified activation functions	5
VII. Demonstration of logical NAND threshold using ReLU activation function	6
VIII. Comparison of discrete and analog thresholds for formula-based computation	8
References	9

### I. DIGITAL FAULT TOLERANCE VIA CONCATENATED REPETITION CODE

We begin by presenting an adaptation of the original construction of a fault-tolerant Boolean gate via a recursive concatenation of repetition codes, initially proposed in [1] and more rigorously discussed in [2]. To best explain this scheme, let us consider a Boolean gate  $B(x)$ , where  $x$  may denote multiple bits (for instance  $\text{NAND}(x_0, x_1)$ ), and its faulty counterpart  $B_p$  that fails (i.e. outputs the incorrect bit) with probability  $p$ . We would like to construct a fault-tolerant version of  $B_p$  whose error can be decreased arbitrarily for  $p < p_0$ . This is achieved by devising a recursive concatenation scheme wherein a *logical*  $B$  gate is constructed from *physical*  $B$  gates, these being the faulty  $B_p$  gates. In particular, a logical  $B$  gate at concatenation level- $\ell$ , which we denote by  $B_p^{(\ell)}$ , is recursively defined by a mapping of gates at concatenation level  $\ell - 1$ , with the base case  $B_p^{(0)}(x) = B_p$ . In this mapping,  $B_p^{(\ell)}$  is defined as a repetition code acting on multiple outputs of  $B_p^{(\ell-1)}$ , such that the error suffered by  $B_p^{(\ell)}$  is less than that of  $B_p^{(\ell-1)}$  for  $p < p_0$ .

In the seminal work on fault tolerance, von Neumann employed a ternary repetition code, in which a logical bit is encoded as a bundle of physical bits. At concatenation

level  $\ell$ , each bundle consists of  $3^\ell$  physical bits, and its corresponding logical bit may be decoded as the majority of its physical bits; for instance, 110 encodes the logical bit 1 at concatenation level  $\ell = 1$ . In this manner, the inputs and outputs to  $B_p^{(\ell)}(x)$  are bundles of size  $3^\ell$ , and the output is correct if its physical bits decode to the correct logical bit.

The recursive mapping from  $B_p^{(\ell)}$  to  $B_p^{(\ell+1)}$  is defined by this ternary repetition code: the inputs to  $B_p^{(\ell+1)}$ , which are bundles of size  $3^{\ell+1}$ , are linearly partitioned into three bundles of size  $3^\ell$ , which are then sent through  $B_p^{(\ell)}$  gates in parallel to generate nine independent output bundles (each also of size  $3^\ell$ ). To correct possible errors in the output bundles, these bundles are then split into three groups of threes, each of which is passed through a (faulty) majority voting gate, and the resulting outputs are recombined into a bundle of size  $3^{\ell+1}$  which represents the final output of  $B_p^{(\ell+1)}$ . The majority voting gate is constructed from  $B_p^{(\ell)}$  gates, and hence is also imperfect; its explicit construction depends on the Boolean gate of interest and influences the fault tolerance threshold. In general, the fewer  $B_p^{(\ell)}$ 's in the majority gate, the larger the threshold.

For clarity, we depict the application of this fault tolerance protocol to a NAND gate in Fig. S1. The specific arrangement of the wires fed into the majority voting gates is chosen to prevent error propagation and produce a nonzero threshold. Not all arrangements will yield a nonzero threshold in the limit  $\ell \rightarrow \infty$ ; von Neumann's original presentation even suggests randomly permuting these wires. As the NAND gate is universal for Boolean computation, this construction enables arbitrarily accurate computation of any Boolean function from faulty NAND gates if the failure probability  $p$  lies below the threshold  $p_0$ .

### II. FAULT TOLERANCE AGAINST SYNAPTIC FAILURE VIA CONCATENATED REPETITION CODE

In this section, we describe the details of how the aforementioned concatenated repetition code may be adapted to devise a fault-tolerant neural network robust against synaptic failure. We consider a neural network constructed from rectified linear unit (ReLU) activation functions, where  $\text{ReLU}(x) = \max(0, x)$  on real inputs  $x$ . In this case, synaptic failure may be modelled by replacing each ReLU with a faulty ReLU that fails with

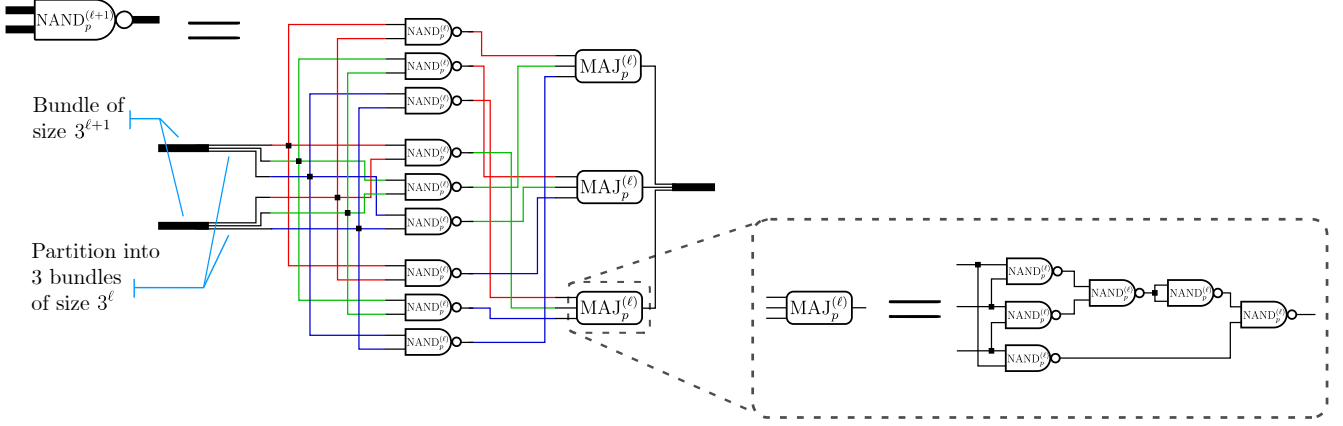


FIG. S1. The recursive concatenation scheme, based on a repetition code, used to construct a NAND at concatenation level  $\ell + 1$  (denoted  $\text{NAND}_p^{(\ell+1)}$ ) from NAND's at level  $\ell$ , with the base case  $\text{NAND}_p^{(0)} = \text{NAND}_p$ . The gates denoted  $\text{MAJ}_p^{(\ell)}$  indicate a majority voting operation, whose construction is illustrated in the inset. Note how the fault-tolerant ReLU of Fig. 2 of the main text is a generalization of this construction.

probability  $p$ :

$$\text{ReLU}_p(x) = \begin{cases} \text{ReLU}(x) & \text{with probability } 1 - p \\ 0 & \text{with probability } p \end{cases} \quad (\text{S1})$$

Like von Neumann's error model for Boolean gates, the output of this faulty ReLU is reliably incorrect with some probability, and thus its errors may be corrected by employing a concatenated repetition code.

The aim is thus to construct a fault-tolerant ReLU activation function, or equivalently a fault-tolerant neuron. We will employ a concatenated ternary repetition code analogous to that presented above, replacing each logical Boolean gate at level  $\ell$  with a logical ReLU at level  $\ell$ , which we denote by  $\text{ReLU}_p^{(\ell)}$ . However, there is one important distinction in our construction: as inputs and outputs are now analog instead of binary, we will interpret the logical value carried by a bundle as the *median* of its values. Accordingly, the majority voting gate in the original repetition code is replaced by a median gate, which will appropriately correct single errors. The complete recursive scheme is depicted in the main text in Fig. 1.

What remains is to construct the median operation out of ReLU's. At concatenation level  $\ell$ , we are interested in computing the median of three bundles, each of size  $3^\ell$ . Denoting this quantity as  $m = \text{Med}_p^{(\ell)}(a, b, c)$ , it may be computed with the following network of depth three:

$$\begin{aligned} x &= \text{ReLU}_p^{(\ell)}(a - b) \\ y &= \text{ReLU}_p^{(\ell)}(-a + c + x) \\ z &= \text{ReLU}_p^{(\ell)}(b - c + x) \\ m &= \text{ReLU}_p^{(\ell)}(a + b - c + y - z). \end{aligned} \quad (\text{S2})$$

While the final ReLU is not strictly necessary for the

computation of the median, it is included to prevent error propagation from the inputs and achieve fault tolerance. As a result, this median works only on positive inputs, but this is admissible as the output of  $\text{ReLU}_p^\ell$  (which is input into the median) is necessarily non-negative. We also note that this median construction employs skip connections to perform its computation.

As demonstrated in the main text, this construction ultimately produces a fault-tolerant ReLU neuron with threshold  $p_0 \approx 3.72\%$ . The straightforward assembly of individual fault-tolerant neurons provides a fault-tolerant neural network protected against synaptic failures.

### III. COMPARISON OF REPETITION FOR DISCRETE VERSUS ANALOG FAULT-TOLERANCE

While the repetition code is sufficient to arrive at digital fault-tolerance when subject to bit-flip errors or synaptic failure, it is insufficient for analog computation in the presence of additive Gaussian noise. Key to this is the  $\mathcal{O}(\text{polylog}(1/\epsilon))$  scaling with respect to the desired output error rate  $\epsilon$  in the definition of fault-tolerance.

For Boolean (more generally discrete) random variables, suffering from i.i.d. bit-flip errors at a rate  $p < 1/2$ , a repetition code of size  $M$  reduces errors exponentially as  $\sim p^M$ . Given a target error rate  $\epsilon$ , it is sufficient to choose

$$M \sim \frac{\log \frac{1}{\epsilon}}{\log \frac{1}{p}}. \quad (\text{S3})$$

Using the concatenation scheme described in Section I and the union bound to reduce errors to  $N/\epsilon$ , we find that this translates to the desired  $\mathcal{O}(N \log^b(N/\epsilon))$  scaling in the definition of fault-tolerance so long as the error rate



is below a threshold  $p_0$  that is dependent on the details of the error correcting circuit.

For analog variables, the repetition code does not suppress errors strongly enough to achieve this scaling. For additive Gaussian noise with standard deviation  $\sigma$ , a repetition code of size  $M$  suppresses errors not exponentially in  $M$ , but only as  $\sim \sigma/\sqrt{M}$ . For a target standard deviation  $\epsilon$ , the code size is required to scale as

$$M \sim \left(\frac{\sigma}{\epsilon}\right)^2. \quad (\text{S4})$$

Analog computation using the repetition code would require an asymptotic lower bound of  $\Omega(\text{poly}(1/\epsilon))$  resources, and thus does not meet our definition of fault-tolerance. In order to achieve analog fault-tolerance, we must make use of a stronger error correcting code.

#### IV. SUMMARY OF GRID CODES

For reference, we will now provide a self-contained exposition of the original grid code results [3–5]. The codespace is defined by a set of  $M$  relatively prime integers (“moduli”) denoted  $\{\lambda_j\}_{j=1}^M$ .

In a noiseless setting, the grid code encoder maps an element  $x_{i_0}$  from a set of discrete values  $\{x_i\}$  over a fixed domain  $0 \leq x_i < X$  to a codeword of phases  $\phi := \text{Enc}[x_{i_0}]$  for encoder

$$\text{Enc}[x_{i_0}] := \left\{ \phi_j = \frac{e(x_{i_0})}{\lambda_j} \bmod 1 \right\}, \quad (\text{S5})$$

where the function  $e(x_{i_0}) \in [0, X)$  is chosen to be the identity to simply represent  $x_{i_0}$ ; we will later choose non-identity  $e$  to perform computation. The choice of relatively prime moduli ensures, by consequence of the Chinese Remainder Theorem, that all  $x \in [0, \prod_{j=1}^M \lambda_j)$  are encoded into distinct codewords. Restricting our domain as above, with  $X \ll \prod_{j=1}^M \lambda_j$ , allows the remaining phase space to be used for error correction. To maintain the favorable error-correcting properties of the grid code, the  $x_i$ ’s are chosen to satisfy  $x_i \ll X$ ; and the minimum spacing between codewords  $\Delta x := \min_{i \neq j} |x_i - x_j|$  is chosen such that  $\max_j \lambda_j \ll \Delta x$ . More generally, when  $e(x_{i_0})$  is not the identity function, the same condition must be upheld for  $\Delta x$  given by  $\min_{i \neq j} |e(x_i) - e(x_j)|$  such that  $e(x_i) \neq e(x_j)$ . In this limit, two codewords encoding randomly sampled  $x_1, x_2 \in [0, X)$  (or  $e(x_1)$  and  $e(x_2)$ ) are well-approximated by i.i.d. samples of a uniform distribution [5].

In the presence of Gaussian neural spiking noise, the noiseless encoder  $\text{Enc}[x_{i_0}]$  is replaced by the noisy encoder

$$\widetilde{\text{Enc}}[x_{i_0}] = \left\{ \tilde{\phi}_j = \frac{e(x_{i_0})}{\lambda_j} + \xi \bmod 1 \right\}, \quad (\text{S6})$$

for i.i.d.  $\xi \sim \mathcal{N}(0, \sigma)$  sampled for each phase.

We now show that the described decoding procedure, illustrated in Fig. 2b of the main text, is indeed performing maximum likelihood estimation. If  $x$  is known to belong to a discrete set of values  $\{x_i\}$ , the estimated decoding  $\hat{x}$  is given by maximizing the conditional probability

$$\hat{x} = \arg \max_{x_k} P(\phi|x_k). \quad (\text{S7})$$

The likelihood function is a wrapped normal distribution

$$P(\phi|x_k) \propto \prod_{j=1}^M \exp\left(-\frac{1}{2\sigma^2} \|\text{Enc}[x_k]_j - \phi_j\|^2\right), \quad (\text{S8})$$

where  $\|x\| \equiv \min\{|x|, 1 - |x|\}$  denotes the distance between phases. The likelihood function is well approximated by the more tractable circular normal function in the limit of  $\sigma \ll 1$  by

$$P(\phi|x_k) \propto \prod_{j=1}^M \exp\left(\frac{1}{2\pi\sigma^2} \cos\left[2\pi\left(\frac{x_k}{\lambda_j} - \phi_j\right)\right]\right). \quad (\text{S9})$$

Comparing Eq. S9 and Eq. 2 in the main text, we see that the neural network is maximizing the likelihood.

We now summarize an analysis of the grid code’s distance. Since the  $M$  phases  $\phi_j$  fall between 0 and 1, the coding space is the unit hypercube  $[0, 1]^M$ ; due to unit modulo, the coding space satisfies periodic boundary conditions and thus corresponds to the  $M$ -torus. The coding line  $[0, X)$  is thus a set of parallel line segments in the hypercube. In general, error correction codes may be described as a hypersphere packing problem: each codeword corresponds to an origin of a sphere in a high-dimensional space, and errors that fall within the radius of the sphere are correctable to the true codeword. Here, the grid code is a hypersphere packing problem in the  $M - 1$  dimensional hyperplane perpendicular to the coding line segments. Under this formalism, we arrive at a scaling of the minimum distance between line segments with the number of phases for fixed  $X$  of  $d_{\min} = \Theta(\sqrt{M})$  [5], denoting an asymptotic bound on  $d_{\min}$  from both above and below. Our choice of  $\lambda \ll \Delta x$  ensures that each  $\text{Enc}[x_i]$  lies within a different line segment and therefore is also separated by at least  $d_{\min}$ , and consequently any perturbation in the phase space less than  $d_{\min}/2$  is correctable using the maximum likelihood decoder.

#### V. FAULT-TOLERANT GAUSSIAN-WEIGHTED NEURAL NETWORK

We now provide details of the computation showing the number of physical neurons required to suppress arbitrary Gaussian noise. We assume an error model where  $\xi \sim \mathcal{N}(0, \sigma)$  is added to the output of each neuron, rep-

representing the noise associated with neural spikes in a biological setting. We will be encoding an  $x_{k_0}$  that is guaranteed to belong to a discrete set of  $S$  values  $\{x_k = k\Delta x\}$  for  $k = 0, \dots, S-1$ , such that  $(S-1)\Delta x < X$  for some  $X$ . The moduli must satisfy  $\lambda_j \ll X \ll \prod_{j=1}^M \lambda_j$  for relatively prime  $\lambda_j$ , and thus  $x_k/\lambda_j \sim \mathcal{U}(0,1)$  for random  $x_k$ . Additionally, we take both the number of moduli  $M$  and the number of neurons  $m_0$  connected from the previous layer to be much larger than one, allowing application of the central limit theorem.

Taking advantage of the periodicity of the grid code due to the periodicity of the phases, we introduce a smaller range of values  $[0, X')$  compared to the full range of the standard grid code  $[0, X)$ . To remain consistent with the assumptions stated above, we require  $\lambda_j \ll X' \ll \prod_{j=1}^M \lambda_j$ . Moreover, in order to maintain properties of modular arithmetic, we restrict the logical weights to integer weights  $a_i \in \mathbb{Z}$  such that  $\sum_i |a_i| \leq X/X'$ . In order to implement a ReLU activation function, we choose the logical activation function

$$e(x_i) = \begin{cases} 0 & (x_i \bmod X') < X'/2 \\ (x_i - X'/2) \bmod X' & (x_i \bmod X') \geq X'/2, \end{cases} \quad (\text{S10})$$

as shown in Fig. S2. This may be implemented by choosing weights on the physical neurons  $W_{ij}^{\text{enc}} = \frac{e(x_i)}{\lambda_j} \bmod 1$  (red connections in Fig. 2a of the main text). However, we assume that the logical weights  $a_i$  are approximately normally distributed from a Gaussian distribution with standard deviation  $\alpha$ . (In Sec. VI, logical weights will be set to unity to implement Boolean gates.)

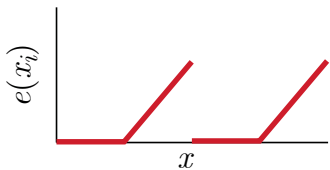


FIG. S2. Rectified linear unit (ReLU) activation function for  $X' = X/2$ . The logical ReLU activation function  $e(x_i)$  used in the encoder (Eq. S10) allows the fault-tolerant neural network to implement the standard ReLU activation function.

The general construction of the logical neuron (Fig. 3a of the main text) is as follows. A previous layer of logical neurons passes to the logical neuron a set of encoded phase vectors, where the  $i$ th input neuron is denoted  $\theta^{(i)}$ . Each input neuron  $\theta^{(i)}$  encodes a quantity that lies in  $[0, X')$  in the decoded space. A series of logical weights are applied, mapping directly from grid code phases to grid code phases. Due to the unit modulo of the grid code, this will ultimately cause a sawtooth-like activation function in the decoded space. Explicitly, this unit modulo is realized by sine and cosine activation functions in the next stage of the logical neuron: the decoder. The decoder has two roles in the logical neuron. Firstly, it

performs error correction, following the grid code formalism described above. Secondly, it performs computation, introducing a nonlinearity via sine and cosine functions that impose the periodicity of the phase encoding. Moreover, the decoder does not return to the original  $[0, X')$  space; instead, it corresponds to the standard grid code decoder over the larger space  $[0, X)$ , allowing the application of logical weights to decode to valid values. In the final stage of the logical neuron, we apply an encoder that returns to  $[0, X')$  by choosing appropriate weights that implement a logical activation function. Consequently, much like the decoder, the encoder both plays a role similar to the original grid code (i.e. taking  $x_i$  to a vector of phases) and is directly involved in the computational aspect of the logical neuron.

Throughout the logical neuron, synaptic failures may occur, increasing the logical error probability of the final output. Although the grid code can correct all analog errors of the form of Gaussian additive noise applied to the neural spiking output, these synaptic failures cannot be reliably corrected. In the standard neural network described in this section, we do not address the synaptic failures. However, in the neural implementation of the NAND gate (Sec. VII), we apply the standard fault-tolerant NAND construction of Evans and Pippenger [6] to correct for synaptic failures. This also provides a reconciliation with von Neumann's traditional approach to fault tolerance, where all computations occur within the codespace: a fully fault-tolerant neural network is achieved by combining the traditional concatenated repetition code and the grid code, ensuring that the computation does indeed remain in a protected codespace throughout the entire computation.

The above framework is now made explicit to demonstrate the fault-tolerant properties of the logical neuron. Working in the codespace, the  $m_0$  neurons from the previous layer connected to the logical neuron are represented by codewords  $\text{Enc}[x_1], \dots, \text{Enc}[x_{m_0}]$ . Letting  $\text{Enc}[x_i] = \{\theta_j^{(i)}\}$  for  $j = 1, \dots, M$ , we must map from the  $m_0 \times M$  neurons in  $\{\text{Enc}[x_i]\}$  to a single set of phases  $\{\phi_j\}$  such that our activation function is applied *after* decoding and re-encoding (since the encoder applies the ReLU activation function). By assigning weights  $W_{ij} = a_i$  from  $\theta_j^{(i)}$  to  $\phi_j$  with a linear activation function and bias  $-\frac{X'}{\lambda_j} \sum_{i:a_i < 0} a_i$ , we obtain phases in the absence of noise:

$$\phi_j = \left( \sum_i a_i \theta_j^{(i)} \right) - \left( \frac{X'}{\lambda_j} \sum_{i:a_i < 0} a_i \right). \quad (\text{S11})$$

Adding in noise, a noisy encoding thus generates phases  $\tilde{\theta}_j^{(i)}$ . Each of the  $S$  neurons over the discretized decoded space have noise  $\xi$ , and each is multiplied by approximately uniformly distributed weights due to the phases over the moduli. Applying the central limit theorem to  $\sum_{i=1}^S u\xi$  for  $u \sim \mathcal{U}(0,1)$ , we find mean zero noise with variance  $\sigma^2 \cdot S/3$ . (For simplicity of notation, we drop the

subscript on each  $\xi$  denoting the i.i.d. random variables.) Adding the noise of the codespace neuron to the noise acquired from the plaintext neuron, we find  $\tilde{\theta}_j^{(i)} = \theta_j^{(i)} + \xi + \zeta$  for  $\zeta \sim \mathcal{N}(0, \sigma\sqrt{S/3})$ . Inserting noise in Eq. S11, we have

$$\begin{aligned} \tilde{\phi}_j &= \left[ \sum_{i=1}^{m_0} a_i \tilde{\theta}_j^{(i)} \right] - \left( \frac{X'}{\lambda_j} \sum_{i:a_i < 0} a_i \right) + \xi \\ &= \phi_j + \xi + \sum_{i=1}^{m_0} a_i (\xi + \zeta). \end{aligned} \quad (\text{S12})$$

Applying the central limit theorem to the noise interacting with the neural network weights  $a_i$ , we find that the mean vanishes and  $\text{Var}[\sum_{i=1}^{m_0} a_i (\xi + \zeta)] = \frac{1}{3} S m_0 \alpha^2 \sigma^2$ . To simplify notation, we introduce the variable  $a = 4\pi^2(1 + S m_0 \alpha^2/3)$ .

The error correction  $\tilde{\phi}' = \widetilde{\text{Enc}}[\widetilde{\text{Dec}}[\tilde{\phi}]]$  will produce the correct codeword with error  $\xi$  on each phase — as was assumed in the logical neuron input — if  $\text{Dec}[\tilde{\phi}]$  identifies the correct value. The decoder shown in Fig. 3a of the main text uses two layers, which we now make explicit. The first layer multiplies each  $\phi_j$  with weight  $2\pi$ ; the second layer uses periodic activation functions to compute  $\sin(2\pi\phi_j)$  and  $\cos(2\pi\phi_j)$  respectively multiplied with weights  $W_{jk}^{\sin} = \sin\left(2\pi\frac{x_k}{\lambda_j}\right)$  and similarly  $W_{jk}^{\cos} = \cos\left(2\pi\frac{x_k}{\lambda_j}\right)$ . After applying the final step activation function to obtain a decoding, the error is ‘reset’ if the decoding  $\widetilde{\text{Dec}}[\tilde{\phi}]$  is successful: the logical neuron will not propagate any additional noise into future computations. Evaluating all noise contributions, we have

$$\text{Dec}[\tilde{\phi}] = \arg \max_k f(k), \quad (\text{S13})$$

$$f(k) := \xi + \sum_{j=1}^M [f_1(j, k) + f_2(j, k)], \quad (\text{S14})$$

where

$$f_1(j, k) = \sin\left(2\pi\frac{x_k}{\lambda_j}\right) \left[ \sin\left(2\pi\tilde{\phi}_j\right) + \xi \right], \quad (\text{S15})$$

$$f_2(j, k) = \cos\left(2\pi\frac{x_k}{\lambda_j}\right) \left[ \cos\left(2\pi\tilde{\phi}_j\right) + \xi \right], \quad (\text{S16})$$

and as usual each  $\xi$  is sampled i.i.d.

Suppose that the correct neuron value corresponds to  $k = k_0$ . For the decoder to identify the correct neuron via a threshold cutoff, we require  $f(k_0) > f(k \neq k_0)$  for all  $k$ . If the mean of the correct neuron is greater than the mean of each incorrect neuron, a threshold will exist to distinguish the correct decoding from incorrect decodings in expectation. We use this to gain an analytical scaling for  $M(\epsilon)$  here; a more detailed treatment of the threshold is found in the analysis of the logical NAND.

The key observation is that the noiseless phases  $\phi_j$  are

given by  $\phi_j = x_{k_0}/\lambda_j \bmod 1$ . At  $k = k_0$ , this phase aligns with the neural network weights  $\sin\left(2\pi\frac{x_{k_0}}{\lambda_j}\right)$  or  $\cos\left(2\pi\frac{x_{k_0}}{\lambda_j}\right)$ . On the other hand, at all  $k \neq k_0$ , the neural network weights are sine or cosine of a uniformly distributed random variable.

Formalizing this argument, we find that the true decoding is centered away from zero:

$$\begin{aligned} f(k_0) &\sim \mathcal{N}\left(Me^{-a\sigma^2/2}, \right. \\ &\quad \left. \sqrt{M\left(\frac{1}{2} + \frac{1}{2}e^{-2a\sigma^2} - e^{-a\sigma^2} + \sigma^2\right) + \sigma^2}\right), \end{aligned} \quad (\text{S17})$$

while the incorrect decoding is centered at zero:

$$f(k \neq k_0) \sim \mathcal{N}\left(0, \sqrt{M\left(\frac{1}{2} + \sigma^2\right) + \sigma^2}\right), \quad (\text{S18})$$

where both distributions are seen to have standard deviations  $\mathcal{O}(\sqrt{M})$ . Upper-bounding the maximum element drawn from the distribution of  $f(k \neq k_0)$  out of  $S$  draws using Jensen’s inequality and a union bound, we find that

$$\begin{aligned} f_{\max}(k \neq k_0) &:= \mathbb{E}[\max \text{draw of } f(k \neq k_0)] \\ &\leq \sqrt{[M(1 + 2\sigma^2) + 2\sigma^2] \log S}. \end{aligned} \quad (\text{S19}) \quad (\text{S20})$$

Finally, to determine if  $\arg \max_k$  returns a value other than  $k_0$ , we compute the probability that this exceeds  $f(k_0)$ :

$$\begin{aligned} \text{Pr}[\text{logical neuron fails}] &= \text{Pr}[f(k_0) < f_{\max}(k \neq k_0)] \\ &\leq \frac{1}{2} \text{erfc} \frac{e^{-a\sigma^2/2} M - \sqrt{[M(1 + 2\sigma^2) + 2\sigma^2] \log S}}{\sqrt{M(1 + e^{-2a\sigma^2} - 2e^{-a\sigma^2} + 2\sigma^2) + 2\sigma^2}}. \end{aligned} \quad (\text{S21})$$

Expanding in small  $\epsilon$  and taking  $M, a\sigma^2 \gg 1$ , we find that

$$\begin{aligned} M(\epsilon) &\approx \log(1/\epsilon) \left[ e^{a\sigma^2} (1 + 2\sigma^2) + e^{-a\sigma^2} - 2 \right] \\ &\approx e^{a\sigma^2} (1 + 2\sigma^2) \log(1/\epsilon), \end{aligned} \quad (\text{S22})$$

consistent with Eq. 7 of the main text. The number of neurons is linear in the number of moduli due to the structure of the logical neuron (see Fig. 3a of the main text).

## VI. DEMONSTRATION OF BOOLEAN GATES WITH MODIFIED ACTIVATION FUNCTIONS

While the neural network presented above is a universal approximator of continuous functions due to the use of a ReLU activation function, we demonstrate the flexibility of the fault-tolerant network construction and

implement different activation functions amenable to the implementation of Boolean gates. (The ReLU neural network is shown to implement Boolean formulas in the following subsection.) By constructing a universal set of Boolean gates with fault-tolerant neural networks, any Boolean circuit can be implemented up to arbitrarily small error in the presence of arbitrarily large noise.

A natural construction for Boolean gates emerges if additional encoders that implement different activation functions are introduced. We will show how to generate the activation functions in Fig. 3b of the main text, which will ultimately allow the neural implementation of a multiplier circuit (Fig. S3 and Fig. 3c).

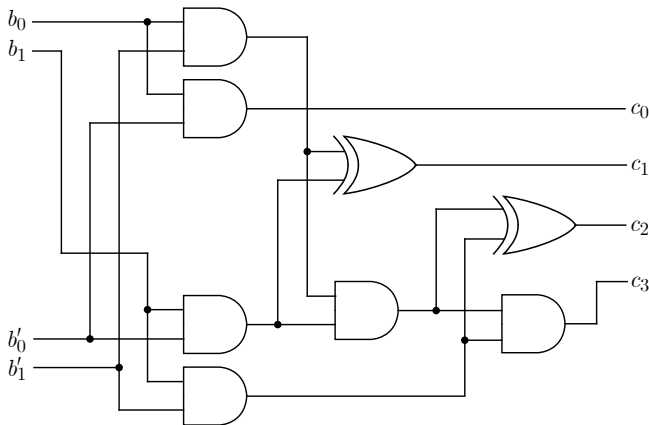


FIG. S3. Two-bit multiplication circuit decomposed into six AND gates and two XOR gates. As shown in Fig. 4 of the main text, a fault-tolerant neural network assembled of neural Boolean gates satisfies the fault-tolerant neural network theorem with  $\mathcal{O}(e^{\mathcal{O}(\sigma^2)})$  physical neurons. Two 2-bit binary numbers  $b_0b_1$  and  $b'_0b'_1$  are provided as input to the circuit, and the output product  $c_0c_1c_2c_3$  is returned. Here, the 0 index denotes the least significant bit.

Define two logical input bits  $A, B \in \{0, a\}$ , interpreting 0 as False and  $a$  as True. Letting  $\Delta x = a$ , the decoder  $\text{Dec}[\phi]$  will only decode to the set of variables  $\{x_1 = 0, x_2 = a, x_3 = 2a\}$ . For notational convenience, we define codeword vectors

$$\phi_a := \left\{ \phi_j = \frac{a}{\lambda_j} \bmod 1 \right\}, \quad (\text{S23})$$

$$\phi_0 := \left\{ \phi_j = \frac{0}{\lambda_j} \bmod 1 \right\}. \quad (\text{S24})$$

Beginning with a NOT gate, define the NOT encoder  $\text{Enc}^\neg[x_1] = \phi_a$  and  $\text{Enc}^\neg[x_2] = \text{Enc}^\neg[x_3] = \phi_0$ . As before, this corresponds to a neural network with weights given by the codeword vectors. To compute  $\neg A$ , we simply compute  $\text{Enc}^\neg[\text{Dec}[A]]$  to apply the error correction and re-encode into the codespace with a NOT computation.

To implement AND and OR gates, we require an additional layer of unity weights, giving  $\phi_i = \theta_i^A + \theta_i^B$ . Ap-

plying the decoder will give either 0,  $a$  or  $2a$  based on the cases  $(A, B) \in \{(0, 0)\}, \{(a, 0), (0, a)\}$  or  $\{(a, a)\}$  respectively. The AND encoder is given by  $\text{Enc}^\wedge[x_1] = \text{Enc}^\wedge[x_2] = \phi_0$  and  $\text{Enc}^\wedge[x_3] = \phi_a$ , and the OR encoder is given by  $\text{Enc}^\vee[x_1] = \phi_0$  and  $\text{Enc}^\vee[x_2] = \text{Enc}^\vee[x_3] = \phi_a$ .

Although AND, OR, and NOT form a universal gate set, we also include XOR for direct use in the two-bit multiplier, given by  $\text{Enc}^\oplus[x_1] = \text{Enc}^\oplus[x_3] = \phi_0$  and  $\text{Enc}^\oplus[x_2] = \phi_a$ . Using these neural gates, we implement the two-bit multiplier shown in Fig. S3.

## VII. DEMONSTRATION OF LOGICAL NAND THRESHOLD USING RELU ACTIVATION FUNCTION

Above, we used natural constructions of Boolean gates through a careful choice of activation function in the codespace. For completeness, we demonstrate here the universality of the fault-tolerant neural network with a ReLU activation function and construct a NAND gate, which allows the implementation of arbitrary Boolean formulas. As seen in the NAND gate activation function of Fig. 3b, the NAND activation function is the opposite of the standard ReLU activation function. Hence, unlike the construction for Boolean formulas described in the previous section, we choose 0 to correspond to the True state and  $a$  to the False state. This makes the ReLU activation function equivalent to the direct implementation of a NAND gate.

Repeating the noisy logical neuron analysis but with logical weights  $a_i = 1$  and three decoder neurons, a similar analysis shows that Eq. S17 is replaced by

$$f_{\text{NAND}}(k_0) \sim \mathcal{N} \left( M \cdot \frac{e^{-6\pi^2\sigma^2} \text{erf}^6(\sqrt{2}\pi\sigma)}{512\pi^3\sigma^6}, \sqrt{M \left( \frac{1}{2} + \sigma^2 - \zeta \right) + \sigma^2} \right), \quad (\text{S25})$$

for

$$\zeta = \frac{e^{-12\pi^2\sigma^2} \text{erf}^{12}(\sqrt{2}\pi\sigma) - 4\pi^3\sigma^6 e^{-24\pi^2\sigma^2} \text{erf}^6(2\sqrt{2}\pi\sigma)}{262144\pi^6\sigma^{12}}. \quad (\text{S26})$$

However, Eq. S18 remains unchanged, i.e.

$$f_{\text{NAND}}(k \neq k_0) \sim \mathcal{N} \left( 0, \sqrt{M \left( \frac{1}{2} + \sigma^2 \right) + \sigma^2} \right). \quad (\text{S27})$$

Repeating the analysis above to estimate  $\Pr[f_{\text{NAND}}(k_0) < f_{\text{NAND}}(k \neq k_0)]$  yields the num-

ber of moduli

$$M(\epsilon) \approx \frac{262144\pi^6 e^{12\pi^2\sigma^2} \sigma^{12} (4\sigma^2 + 1) \log\left(\frac{3}{\epsilon}\right)}{\text{erf}^{12}(\sqrt{2\pi}\sigma)} \quad (\text{S28})$$

$$= \mathcal{O}\left(e^{a\sigma^2} \log(1/\epsilon)\right), \quad (\text{S29})$$

consistent with the result for a Gaussian-weighted neural network.

Establishing maximum neural connectivity simply amounts to requiring  $M \leq M_0$  for fixed  $M_0$ . This limits the amount of Gaussian noise that can be corrected, since the moduli cannot be arbitrarily increased. Additionally, to account for synaptic failure with probability  $p$ , modifications are required for Eqs. S25 and S27. While a functional synapse with additive Gaussian neural spiking error returns value  $y + \xi$ , a synaptic failure returns value 0. We proceed to treat each case of the effect of synaptic failure for each possible type of synapse in Fig. 3a of the main text. The goal is to find an upper bound on the probability that the logical NAND fails, corresponding to a lower bound on the threshold for synaptic failure.

Considering the synapses from the decoder neurons  $x_i$  to the new logical phases  $\phi_j$  (i.e. the final layer of Fig. 3a, a failed synapse may originate from the correct decoder neuron or an incorrect decoder neuron. We ignore the failed synapse from an incorrect decoding, consistent with upper-bounding the failure probability. If the correct decoding fails, the encoded phase may not fire. In the application of logical weights to the logical phase of the next neuron (i.e. the first layer of Fig. 3a), the synapse with a logical weight  $a_i$  may similarly fail. The two phenomena of a correct decoder synapse failing and a logical weight synapse failing produce the same outcome: an input phase  $\theta_i^{(1,2)}$  may fail. The effect of only a single input phase (e.g.  $\theta_i^{(1)}$ ) failing is different from the effect of both input phases failing (i.e.  $\theta_i^{(1)}$  and  $\theta_i^{(2)}$ ). If one input phase fails, the logical phase  $\phi_i$  assumes a uniformly random value from 0 to 1. This has no impact on  $f_{\text{NAND}}(k \neq k_0)$ , but it reduces the mean of  $f_{\text{NAND}}(k = k_0)$  by removing a modulus and requires adjustment of the standard deviation by the inclusion of a random phase. If both input phases fail, the logical phase does not fire. Hence, a modulus is removed from both  $f_{\text{NAND}}(k \neq k_0)$  and  $f_{\text{NAND}}(k = k_0)$ . In total,  $4Mp(1-p)$  single input phases are expected to fail and  $2Mp^2$  double input phases are expected to fail.

Consider the synapses into and out of the  $\sin 2\pi\phi_i$  and  $\cos 2\pi\phi_i$ . Here, we also find two cases: if there is a failure of a single sine or cosine, the original distribution must be compensated by the remaining sine or cosine of the phase; if there is a failure of both, the modulus is removed entirely. In expectation,  $2Mp(1-p)$  failures are expected for the former effect (for each of sine and cosine), and  $2Mp^2$  failures are expected for the latter.

By adding each of the failure modes independently, we place an upper bound on logical failure due to double-

counting failures that happen sequentially in the network. To evaluate the final distributions  $f'_{\text{NAND}}(k \neq k_0)$  and  $f'_{\text{NAND}}(k = k_0)$  that account for synaptic failure, we assume a large number of moduli  $M \gg 1$  and apply the central limit theorem. This produces a new set of distributions, e.g.

$$f'_{\text{NAND}}(k \neq k_0) = \mathcal{N}\left(0, \sqrt{\sigma^2 - \frac{1}{2}M(2p(p+1) - 1)(2\sigma^2 + 1)}\right). \quad (\text{S30})$$

We now provide a more careful treatment of the activation function required for the error correction step of the logical neuron. In a biological discussion of the grid code, winner-take-all dynamics are often used to describe the decoding process [5]. However, for transparency in the treatment of noise, we demonstrate how a step activation function can replace winner-take-all dynamics with a simpler decoder.

Since  $f'_{\text{NAND}}(k \neq k_0)$  is centered at zero with standard deviation  $\mathcal{O}(\sqrt{M})$ , and  $f'_{\text{NAND}}(k = k_0)$  is centered at  $\mathcal{O}(M)$  with standard deviation  $\mathcal{O}(\sqrt{M})$ , we may choose a cutoff  $c$  that maximizes the probability of distinguishing between correct and incorrect decodings. Since there are three decoding neurons, a correct decoding requires the two incorrect neurons sampled from  $f'_{\text{NAND}}(k \neq k_0)$  to lie below  $c$  and the correct neuron to sampled from  $f'_{\text{NAND}}(k = k_0)$  to exceed  $c$ . Evaluating such probabilities is straightforward due to  $f'_{\text{NAND}}$  being normally distributed in both cases. This is performed analytically in Fig. 4a for the dashed line, while the cutoff is estimated numerically in the shaded region.

Evaluated explicitly in terms of neural spiking noise standard deviation  $\sigma$  and probability of synaptic failure  $p$ , the probability that the logical NAND neuron succeeds is given by

$$\frac{1}{8} \left( \text{erf}\left(\frac{c}{\sqrt{2\sigma^2 - M(2p(p+1) - 1)(2\sigma^2 + 1)}}\right) + 1 \right)^2 \times \text{erfc}\left\{ \left( 512\pi^3 c \sigma^6 - e^{-6\pi^2\sigma^2} M(2(p-3)p+1) \text{erf}\left(\sqrt{2\pi}\sigma\right)^6 \right) / \left[ - \left( 2M(p(3p-7) + 1) e^{-24\pi^2\sigma^2} \left( e^{12\pi^2\sigma^2} \times \text{erf}\left(\sqrt{2\pi}\sigma\right)^{12} - 4\pi^3\sigma^6 \text{erf}\left(2\sqrt{2\pi}\sigma\right)^6 \right) \right) - 262144\pi^6\sigma^{12} (M(2p(p+1) - 1)(2\sigma^2 + 1) - 2\sigma^2) \right]^{1/2} \right\}, \quad (\text{S31})$$

where the decoding step activation function cutoff  $c$  is obtained by maximizing the probability of success over all possible values of  $c$ . To obtain the fault-tolerance threshold in Fig. 4a, we apply the result of Evans and Pippenger [6] for fault-tolerant Boolean formulas of NAND

gates, which are possible if and only if the NAND probability of failure is below  $\epsilon_0 = (3 - \sqrt{7})/4$ . Accordingly, the quantity in Eq. S31 is compared to the threshold at  $M = 10^5$  (per the neural connectivity constraint of Purkinje cells [7]), allowing a threshold contour to be determined in  $\sigma$  and  $p$ .

### VIII. COMPARISON OF DISCRETE AND ANALOG THRESHOLDS FOR FORMULA-BASED COMPUTATION

Finally, we analyze a simple analog model of Boolean formula-based fault-tolerant computation which establishes a baseline for comparing discrete and analog thresholds. This is independent of neural computation, but rather serves as a pedagogical comparison of digital and analog computation that allows analog Gaussian noise to be translated into the well-known failure probability thresholds of Evans and Pippenger [6] using 2-input NAND gates. Accordingly, the thresholds found below do not correspond to fault-tolerant neural network thresholds.

For the following analysis, we consider a binary alphabet encoded into real-valued signals  $\{-1, 1\}$  corresponding to the Boolean 0 and 1 respectively. For convenience we define the Boolean NAND to operate on our alphabet, and therefore it can be viewed as a function  $\text{NAND} : \{-1, 1\} \times \{-1, 1\} \rightarrow \{-1, 1\}$ . There is considerable freedom in defining the analog NAND gate. We will choose to analyse the noise thresholds of two representative candidates, dNAND and aNAND defined below, and argue that these are extremal in the sense that all other reasonable definitions of the analog NAND result thresholds intermediate to the ones presented.

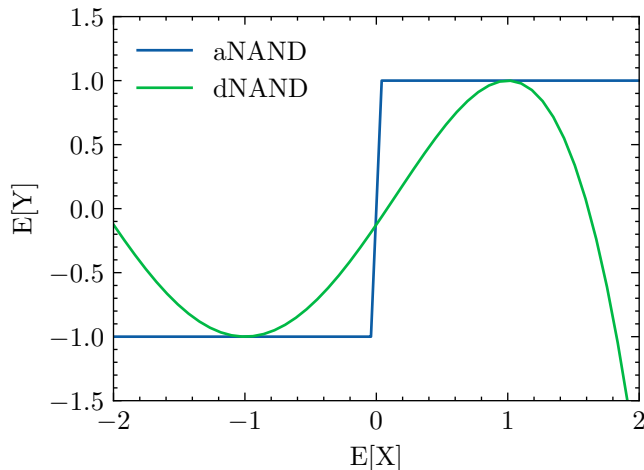


FIG. S4. A comparison of the denoiser response derived from the two proposed analog NAND gates.

First, consider the dNAND defined as follows:

$$\text{dNAND}_\sigma(x, y) := \text{NAND}(\text{sgn}(x), \text{sgn}(y)) + \xi, \quad (\text{S32})$$

where NAND is the noiseless Boolean NAND defined above, and sgn is the sign function. One can verify that a formula composed of dNAND gates works exactly a discrete NAND with an effective error rate  $\epsilon = \Pr[\xi \geq 1]$ . Therefore denoising is successful as long as

$$\frac{1}{2} \left[ 1 - \text{erf} \left( \frac{1}{\sigma\sqrt{2}} \right) \right] < \epsilon_0, \quad (\text{S33})$$

where  $\epsilon_0 = \frac{3-\sqrt{7}}{4}$  denotes the threshold of [6]. Numerically, we find a corresponding analog threshold of  $\sigma < \sigma_d^*$  for  $\sigma_d^* \approx 0.7409$ .

For comparison, consider the aNAND gate defined as follows:

$$\text{aNAND}_\sigma(x, y) := \frac{1 - x - y - xy}{2} + \xi \quad (\text{S34})$$

where  $\xi \sim \mathcal{N}(0, \sigma^2)$ . Note that for  $\sigma = 0$  the analog NAND gate behaves as a noiseless NAND. In this notation, the balanced depth-2 binary tree denoiser used by Evans and Pippenger [6] is written

$$\begin{aligned} \text{Denoise}_\sigma(x_1, x_2, x_3, x_4) = \\ \text{aNAND}_\sigma(\text{aNAND}_\sigma(x_1, x_2), \text{aNAND}_\sigma(x_3, x_4)). \end{aligned} \quad (\text{S35})$$

We would like to analyze the behavior of the denoiser for real-valued i.i.d. random variables  $X_i$  with  $\mathbb{E}[X_i] = x \in \{-1, 1\}$  and  $\text{Var}(X_i) = \alpha^2$ . Define  $Y := \text{Denoise}_\sigma(X_1, X_2, X_3, X_4)$ ; note that  $\mathbb{E}[Y]$  is a quartic polynomial in  $x$  plotted in Fig. S4. One finds that the denoising operation is unbiased (i.e.  $\mathbb{E}[Y] = x$ ) and has variance that depends on  $x$ : for  $x = -1$ ,

$$\text{Var}(Y) = \frac{1}{64} (\alpha^8 + 8\alpha^4 (\sigma^2 + 4) + 16\sigma^2 (\sigma^2 + 12)), \quad (\text{S36})$$

and for  $x = +1$ ,

$$\text{Var}(Y) = \frac{1}{64} (\alpha^4 + 8\alpha^2 + 4\sigma^2)^2 + \sigma^2. \quad (\text{S37})$$

Denoising is successful if  $\text{Var}(Y) < \alpha^2$  for  $x \in \{-1, 1\}$ . As in the discrete case, for  $\sigma < \sigma'_a$ , the denoiser has two fixed points, with the lower one being stable. At the denoising threshold, a saddle-node bifurcation occurs and denoising is no longer possible. Numerically, we find the denoising threshold for the aNAND to be at  $\sigma'_a \approx 0.3929$ . For fault-tolerant computation, we require not only that denoising can be done successfully, but that at least one step of computation can be applied between denoising stages without exceeding the capacity of our denoiser. In terms of the denoising fixed points, we require that a single aNAND gate with input variances near the lower fixed point produces a resulting value that below the up-

per fixed point. The critical case is that where aNAND is given inputs of opposite value. Numerically we find that computation is possible below  $\sigma_a^* \approx 0.3385$ .

As in the discrete case, computation below threshold is possible with minimal overhead. Since we are assuming a formula-based model of computation, the overhead in question corresponds to an increase in depth. To arrive a rough estimate of the overhead required for denoising, note that the distance between the upper and lower fixed points for gate noise  $\sigma$  below threshold is  $\Theta(\sigma_a^{*2} - \sigma^2)$ ; additionally, each denoising step reduces the variance by

a factor  $1 - \Theta(1)$ . Therefore, we find a modest depth increase by factor

$$L_a = \Theta\left(\frac{1}{\sigma_a^{*2} - \sigma^2} \log\left(\frac{1}{\sigma_a^{*2} - \sigma^2}\right)\right), \quad (\text{S38})$$

which establishes a fault-tolerance theorem for Boolean formulas composed of noisy analog NAND gates and is a similar form to the factor found by Evans and Pippenger [6] for the case of computation with discrete NAND gates.

- 
- [1] J. von Neumann, “Probabilistic logics and the synthesis of reliable organisms from unreliable components,” in *Automata Studies. (AM-34), Volume 34*, edited by C. E. Shannon and J. McCarthy (Princeton University Press, 2016) pp. 43–98.
- [2] S. Winograd and J. D. Cowan, *Reliable computation in the presence of noise* (MIT Press Cambridge, Mass., 1963).
- [3] T. Hafting, M. Fyhn, S. Molden, M.-B. Moser, and E. I. Moser, *Nature* **436**, 801 (2005).
- [4] I. R. Fiete, Y. Burak, and T. Brookings, *Journal of Neuroscience* **28**, 6858 (2008).
- [5] S. Sreenivasan and I. Fiete, *Nature Neuroscience* **14**, 1330 (2011).
- [6] W. Evans and N. Pippenger, *IEEE Transactions on Information Theory* **44**, 1299 (1998).
- [7] R. M. A. Napper and R. J. Harvey, *Journal of Comparative Neurology* **274**, 168 (1988).